SCIENTIFIC REPORTS

OPEN

SUBJECT AREAS:
POLYMER CHEMISTRY
IMAGING TECHNIQUES
MATERIALS SCIENCE
SENSORS

Received
21 August 2012

Accepted
27 September 2012

Published
24 October 2012

Correspondence and requests for materials should be addressed to Q.Y. (yangqiong@iccas.ac.cn) or S.W. (wangshu@iccas.ac.cn)

Polymer-drug conjugates for intracellar molecule-targeted photoinduced inactivation of protein and growth inhibition of cancer cells

Bing Wang, Huanxiang Yuan, Chunlei Zhu, Qiong Yang, Fengting Lv, Libing Liu & Shu Wang

Beijing National Laboratory for Molecular Sciences, Key Laboratory of Organic Solids, Institute of Chemistry, Chinese Academy of Sciences, Beijing 100190, P. R. China.

For most molecule-targeted anticancer systems, intracellular protein targets are very difficult to be accessed by antibodies, and also most efforts are made to inhibit protein activity temporarily rather than inactivate them permanently. In this work we firstly designed and synthesized multifunctional polymer-drug conjugates (polythiophene-tamoxifen) for intracellular molecule-targeted binding and inactivation of protein (estrogen receptor α, ERα) for growth inhibition of MCF-7 cancer cells. Small molecule drug was conjugated to polymer side chain for intracellular signal protein targeting, and simultaneously the fluorescent characteristic of polymer for tracing the cellular uptake and localization of polythiophene-drug conjugates by cell imaging. Under light irradiation, the conjugated polymer can sensitize oxygen to produce reactive oxygen species (ROS) that specifically inactivate the targeted protein, and thus inhibit the growth of tumor cells. The conjugates showed selective growth inhibition of ERα positive cancer cells, which exhibits low side effect for our intracellular molecule-targeted therapy system.

Signal pathways are responsible for most biological processes such as cell growth, differentiation, migration and apoptosis. Abnormal expression of proteins corresponding to specific signal pathway is closely related with many serious diseases, especially cancer[1–3]. In recent decades, advances in genomics, proteomics, chemistry, and protein engineering coalesce to accelerate the development of targeted anticancer drugs[4–6]. In these studies, small molecule drug-antibody conjugates that target specific proteins to retard cancer cell signal transduction to arrest tumor growth are most favored as a result of relatively low side effect and strong selectivity. However most efforts are made to inhibit protein activity temporarily rather than inactivate them permanently. In the latter case, the protein remains inactive after the inhibitor diffuses away, and thus enhanced drug potency can be achieved.

Photodynamic therapy (PDT) has been widely used for various cancer treatments to kill tumor cells[7]. The cytotoxic agents, reactive oxygen species (ROS), are generated from the photosensitizer excited by appropriate light exposure. With the interactions between ROS and biomacromolecules, tumor cell apoptosis and necrosis can be initiated. Nevertheless, the surrounding healthy tissues are damaged at the same time. To minimize the side effects of conventional PDT, molecule-targeted PDT systems have been developed, yet with limited success[8–12]. In these systems, proteins targeted by antibodies or small molecules can be selectively inactivated by ROS generated by photosentizers under light, without affecting the surrounding biomolecules. These systems combine the benefits of targeting and inactivating and exhibit high spatial and temporal resolution in a noninvasive manner. However, these systems have two limitations: 1) proteomic or genetic modification is always needed[9]; 2) intracellular targets cannot be accessed by antibodies without microinject[13]. To the best of our knowledge, although selective photo-inactivation of proteins was studied[8,9,13–17], selective inactivation of intracellar signal protein for cell growth inhibition and cancer treatment is seldom reported.

With the aim to develop a new molecule-targeted PDT system that can selectively target and kill the intracellular signal protein that tumor relies on efficiently with very low side effect, in this work, we designed multifunctional conjugated polymer-drug conjugates (**PTD** and **PTDP**, see their chemical structures in **Figure 1A**). Small molecule drug was conjugated to polymer side chain for intracellular signal protein targeting. The mean particle sizes of **PTD** and **PTDP** are 31 and 83 nm from dynamic light scattering (DLS) experiments, respectively

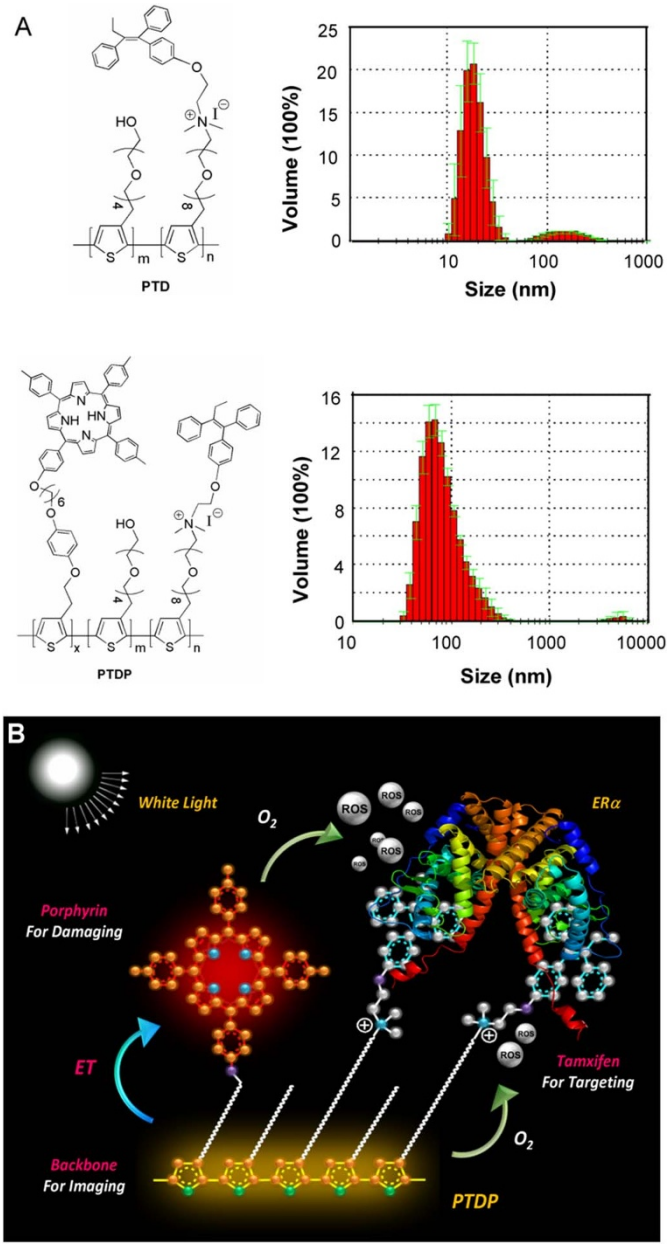

Figure 1 | (A) Chemical structures of conjugated polymer-drug conjugate **PTD** and **PTDP**, and dynamic light scattering analysis (DLS) of their aggregates in aqueous solution. (B) Schematic mechanism of **PTDP** for selective targeting and inactivation of intracellular estregen signal pathway protein.

(as shown in **Figure 1A**), which is in favor of the endocytosis[18]. With light irradiation, the conjugated polymer can sensitize oxygen to produce ROS[12,17,19–23] that specifically inactivate the targeted protein, and thus selectively inhibit the growth of tumor cells. The fluorescent properties of these conjugates can also serve to trace the cellular uptake and localization at different time points by fluorescence imaging. To the best of our knowledge, this is the first polymer/drug/photosensitizer conjugate by the special design and synthesis for intracellular molecule-targeted photodynamic therapy that combines intracellular targeting of a particular protein (estrogen receptor) and its photoinduced inactivation[8,24].

Results

The mechanism of our new conjugated polymer-drug conjugates (**PTD** and **PTDP**) for selective targeting and inactivation of intracellular signal protein is shown in **Figure 1B**. The estrogen receptor α (ERα) can be activated by estrogen, which mediates nuclei receptor signal pathways and influences cell growth and proliferation. Estrogen-mediated growth of human tumors (such as breast tumor) can be inhibited by inactivating ERα using antiestrogen drugs[24,25]. Tamoxifen (**TAM**), the most widely used estrogen receptor modulator[26–28], was linked to side chains of **PTD** and **PTDP** via an oligo-ethyleneglycol (OEG) linker. It was reported that the permanently charged tamoxifen derivatives can decrease side effects, display good affinity to ERα and still modulate ERα-mediated transcription[28]. It is expected that similar modification of tamoxifen to **PTD** and **PTDP** would not deprive the activity of tamoxifen. Under white light irradiation, the conjugated polymer **PTD** can sensitize oxygen to produce ROS that specifically inactivated the targeted ERα protein, retard the estrogen signal pathway and selectively inhibit the growth of the signal pathway relied breast tumor cells. Covalent attachment of porphyrin moieties to the light harvesting backbone of **PTD** yields conjugate **PTDP**, which constrains interchromophore distances for optimizing energy transfer (ET) from polythiophene to porphyrin. This design can increase the ROS generation efficiency and reduce light intensity and polymer concentration requirements[12,22]. Furthermore, the fluorescent properties of the conjugated polymers can also serve to trace the cellular uptake and localization at different time points by fluorescence imaging.

Figure 2 shows the synthesis of **PTD**, **PTDP** and a cationic polythiophene derivative **PTN** using OEG modified thiophene monomer. Reaction of 2-(thiophen-3-yl)ethanol (**1**) and 4-methylbenzene-1-sulfonyl chloride in the presence of pyridine in CH_2Cl_2 affords 2-(thiophen-3-yl)ethyl 4-methylbenzenesulfonate (**2**) in 95% yield. Treatment of **2** with sodium hydride and tetraethylene glycol in anhydrous THF provides compound **3** in 20% yield. Compounds **4** and **6** were prepared by similar procedure as compound **2** in 80% and 95% yields, respectively. Compound **5** was obtained by similar procedure as compound **3** in 50% yield. Treatments of **6** with LiBr and NaI in acetone provide monomer **7** and **8** in 40% and 85% yields, respectively. Monomers **3** and **8** undergo oxidative copolymerization under nitrogen in the presence of $FeCl_3$ to give polythiophene derivative **9** in 39% yield. Subsequent conversion to cationic polymer **PTN** is accomplished in 94% yield by reaction with excess trimethylamine in methanol. Modification of polymer **9** with tamoxifen affords **PTD** in 95% yield. The actual tamoxifen content was determined to be ~60% from ^{1}H NMR spectra. Oxidative copolymerization of monomers **3**, **7** and **10**[12] under nitrogen in the presence of $FeCl_3$ gives polythiophene derivative **11**, followed by modification with tamoxifen and purification by dialysis in water to afford **PTDP** in 36% yield. The actual tamoxifen and porphyrin contents were determined to be ~47% and 3.5%, respectively from ^{1}H NMR spectra. Due to the amphiphilic character, **PTD** and **PTDP** form aggregates in water. By DLS experiments, the mean particle sizes of **PTD** and **PTDP** are 31 and 83 nm, respectively (as shown in **Figure 1A**), which are in favor of the endocytosis[18].

The UV-vis absorption spectrum of control polymer **PTN** exhibits maximum peak at 410 nm, while **PTD** has an additional peak below 300 nm that originates from tamoxifen. The UV-vis absorption spectrum of **PTD** shows a maximum peak at 423 nm in water with a quantum yield of 6% with quinine bisulfate as the standard. The fluorescent property of **PTD** can be used for tracing the cellular uptake and localization. The absorption spectrum of **PTDP** exhibits a peak below 300 nm, a sharp peak at 420 nm and Q bands between 520 nm and 670 nm, which corresponds to tamoxifen, the polymer backbone and porphyrin units. For monomer **10**, the absorption spectrum exhibits a Soret band at 416 nm and Q bands between 520 nm and 670 nm; the emission spectrum shows a maximum peak at 653 nm (**Figure 3A**) with an excitation of 420 nm and there is very low fluorescence excited by 450 nm and 470 nm. Excitation of **PTDP** at 450 or 470 nm, where the porphyrin units do not exhibit

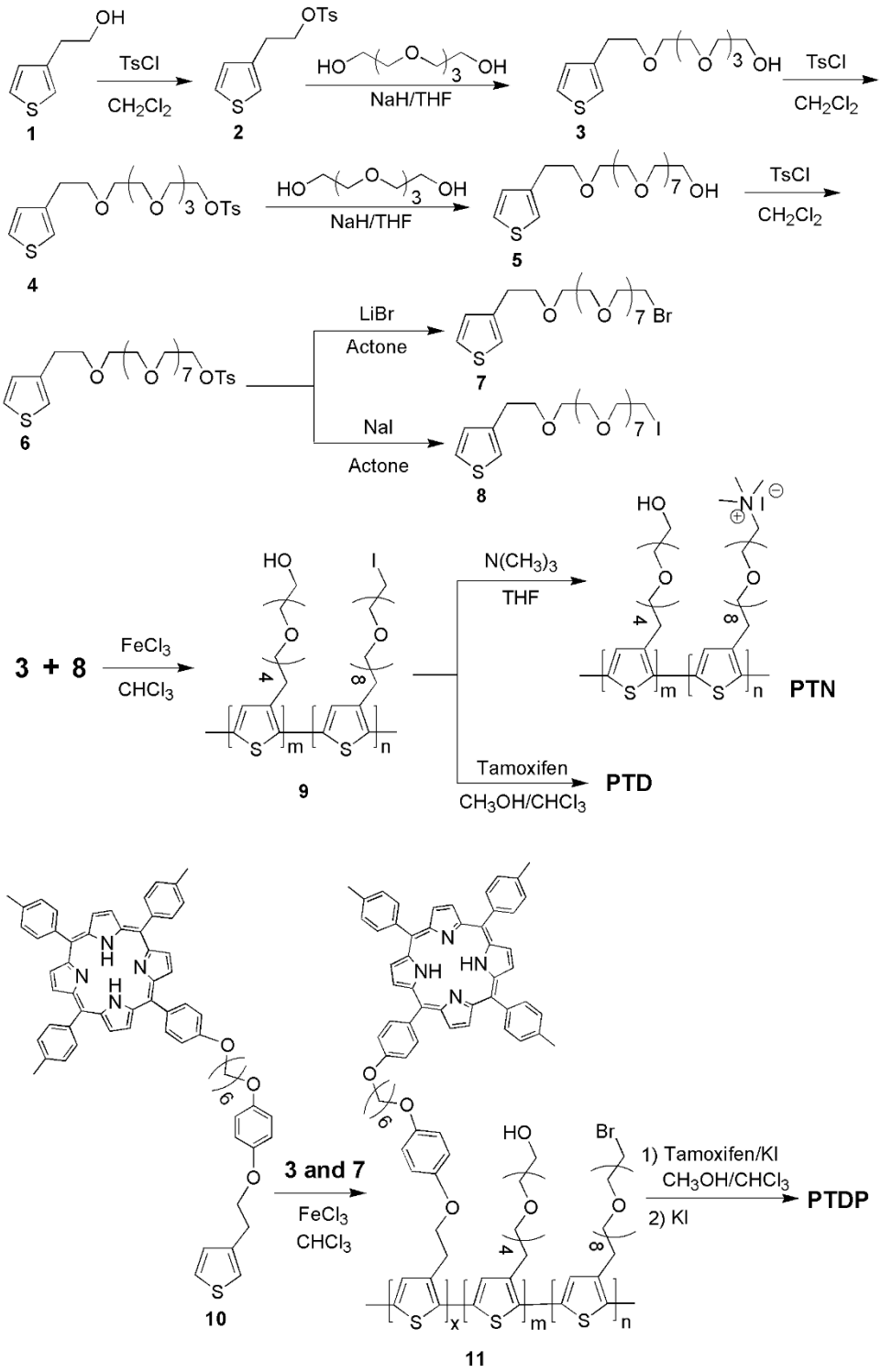

Figure 2 | **Synthetic routes of PTN, PTD and PTDP.**

absorption, leads to emission with peaks at 578 nm and 658 nm. The peak at 658 nm demonstrates efficient energy transfer from polythiophene units to the porphyrin sites (**Figure 3B**). To verify the ROS producing abilities by **PTD** and **PTDP**, 2,7-dichloriflurescin-diacetate (DCFH-DA) was used for semi-quantitative analysis. After conversion of DCFH-DA into 2,7-dichloriflurescin (DCFH), DCFH can transform into highly fluorescent 2,7dichlorofluorescein (DCF) in the presence of ROS[22]. In these experiments, the concentrations of **PTD** and **PTDP** were 5.0 μM in repeat units (RUs), and the concentration of monomer **10** (0.2 μM) matched that of the porphyrin units in the **PTDP** solutions was also measured for comparison. As shown in **Figure 4**, linear relations between the fluorescent intensity of DCF at 530 nm and irradiation time were observed for monomer **10**, **PTD** and **PTDP**, respectively. The slope of **PTDP** is 2 times larger than that of **PTD** and 8 times larger than that of monomer **10**. Thus **PTDP** with porphyrin moieties as side chains thus significantly increases the ROS generation relative to the isolated **PTD** and monomer **10** due to the efficient energy transfer from the polythiophene backbone to the porphyrin sites.

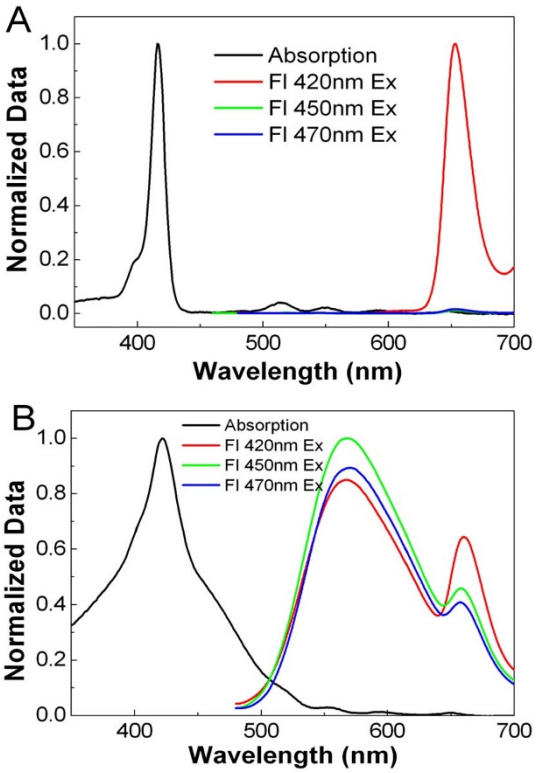

Figure 3 | Normalized UV-vis absorption and fluorescent emission spectra of monomer 10 (A) and PTDP (B) with excitations of 420 nm, 450 nm and 470 nm. [**PTDP**] = 5.0 μM in RUs, [**10**] = 0.2 μM.

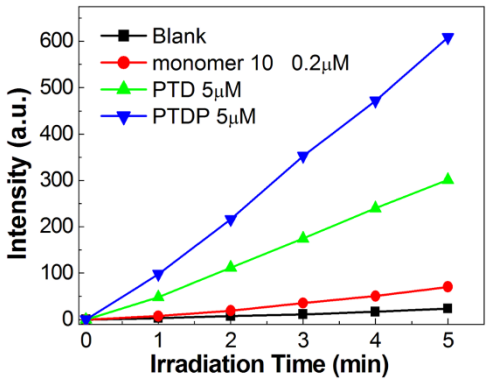

Figure 4 | DCF emission intensity at 530 nm as a function of light irradiation time in aqueous solution in the presence of monomer 10, PTD, and PTDP. [**PTD**] = [**PTDP**] = 5.0 μM in RUs, [**10**] = 0.2. The fluence rate of white light (400–800 nm) is 10 mW·cm^{-2}.

Discussion

PTD was firstly studied for cell imaging. The distribution of **PTD** in ERα positive cell line MCF-7 was traced using fluorescence microscope. CLSM study showed the cellular uptake and localization of **PTD** at different time points (**Figure 5A**). After 2 h incubation with **PTD**, significant uptake in MCF-7 cells was observed and **PTD** mainly located the same place with lysosome stain Lyso Traker DND 99, which revealed the endocytosis process of **PTD**. After 18 h, more polymers escaped from the lysosome, which is in accordance with the reports that polythiophene are usually dispersed in cytoplasm nonspecifically. PTD was further tested on the ERα positive cell line MCF-7 to study the influence of cell proliferation and thus verify the targeting effect. A standard assay was used in which the conversion of MTT (3-(4,5-dimethylthiazol-2-yl)-2,5-diphenyl-2H-tetrazolium hydrobromide) into formazan is related to mitochondrial activity and thereby cell viability. Control experiment indicates that **PTN** shows low toxicity to MCF-7 cells with the concentration up to 100 μM. For **PTD**, the cell viability of MCF-7 tumor cells decrease in a concentration dependent manner (**Figure 5B**). The different concentrations of tamoxifen in **PTD** can be calculated (**Figure 5C**). At the same effective concentration of tamoxifen, polymer-tamoxifen conjugate (**PTD**) exhibits significantly enhanced cell growth inhibition in comparison with tamoxifen itself. Two possible reasons may result in the enhanced cell growth inhibition. Firstly, the polymer–drug system with an appropriate size in nanometer scale (31 nm) that can be endocytosed and enriched in tumor cells. Secondly, local high concentration of tamoxifen in polymer can enhance its binding ability to target protein, ERα.

ERα-mediated transcription was analyzed to further confirm the efficient targeting effect of **PTD**. Tamoxifen inhibits the regulation of specific gene by estrogen and the same inhibition of **PTD** was expected. We know that the binding effect of 17-β-estrodiol to ERα is about 1000 times more powerful than tamoxifen, and the tamoxifen-induced mRNA expression should be reversed with incubation with 17-β-estrodiol. As shown in **Figure 5D**, expression of estrodiol-responsive gene pS2 and PDZK1 was found to be repressed by **PTD**. The mRNA expression of the three genes is about two thirds relative to the control. It is noted that the mRNA expression of pS2 and PDZK1 was recovered after the addition of 17-β-estrodiol 10 hours before cell lysis (**Figure 5E**). The reversible suppression of mRNA transcription confirms that PTD can target ERα and inhibit estrogen-induced activity of ERα.

As shown in **Figure 4**, **PTD** possess the ability to sensitize oxygen to generate ROS under light irradiation due to its conjugated backbone. We subsequently studied whether **PTD** could inactive the targeted ERα and thus enhance the growth inhibition of ERα positive cells. Cytotoxicity experiments on **PTD**, **PTN** and tamoxifen were carried out with white light irradiation at fluence rates of 2 mW·cm^{-2} for 30 min (3.6 J·cm^{-2}) and 8 mW·cm^{-2} for 30 min (14.4 J·cm^{-2}). The control experiments show that **PTN** and tamoxifen exhibit no further cytotoxicity under white light irradiation even at the fluence rate of 8 mW·cm^{-2} (**Figure 6A and 6B**). As shown in **Figure 6C**, **PTD** exhibits little further cytotoxicity under white light irradiation at a fluence rate of 2 mW, nevertheless it displays significantly enhanced cytotoxicity by irradiated at the fluence rate of 8 mW·cm^{-2}. However, the growth of the MCF-7 cells is affected at higher fluence rate irradiation (8 mW·cm^{-2}). Since the **PTDP** with porphyrin moieties as side chains can significantly increase the ROS generation efficiency relative to **PTD**, MCF-7 cells treated with **PTDP** displays quite remarkable sensitivity to light irradiation as expected. As shown in **Figure 6D**, the inhibition of cell proliferation under light irradiation at a fluence rate of 2 mW·cm^{-2} was greatly enhanced than that under dark. We summarized the cell viability of **PTD** and **PTDP** in different conditions (**Table 1**), which shows that **PTDP** exhibits better inhibition activity to cell growth even at lower concentration and light fluence rate in comparison to **PTD**. It is noted that PTDP shows little cytotoxicity towards the ERα negative MDA-MB-231 cells under white light irradiation at a fluence rate of 2 mW·cm^{-2} (**Figure 6E**). In this case, PTDP diffuses in the cytoplasm randomly and the generated ROS spreads quickly and may only cause weak collateral damage. Thus, cell growth inhibition was achieved by selectively retarding the intracellar signal transduction pathway using polymer-drug conjugates. We further studied whether 17-β-estrodiol was able to reverse the irradiation-induced growth inhibition, since excess 17-β-estrodiol can reduce the target effect of tamoxifen and protect the ERα from ROS damaging. As shown in **Figure 6F**, the growth of MCF-7 cells was inhibited after **PTDP** treatment, and the inhibition was reversed when 17-β-estrodiol was added to the culture medium 2 h before light irradiation. The selective inactivation of intracellar signal protein for cell growth

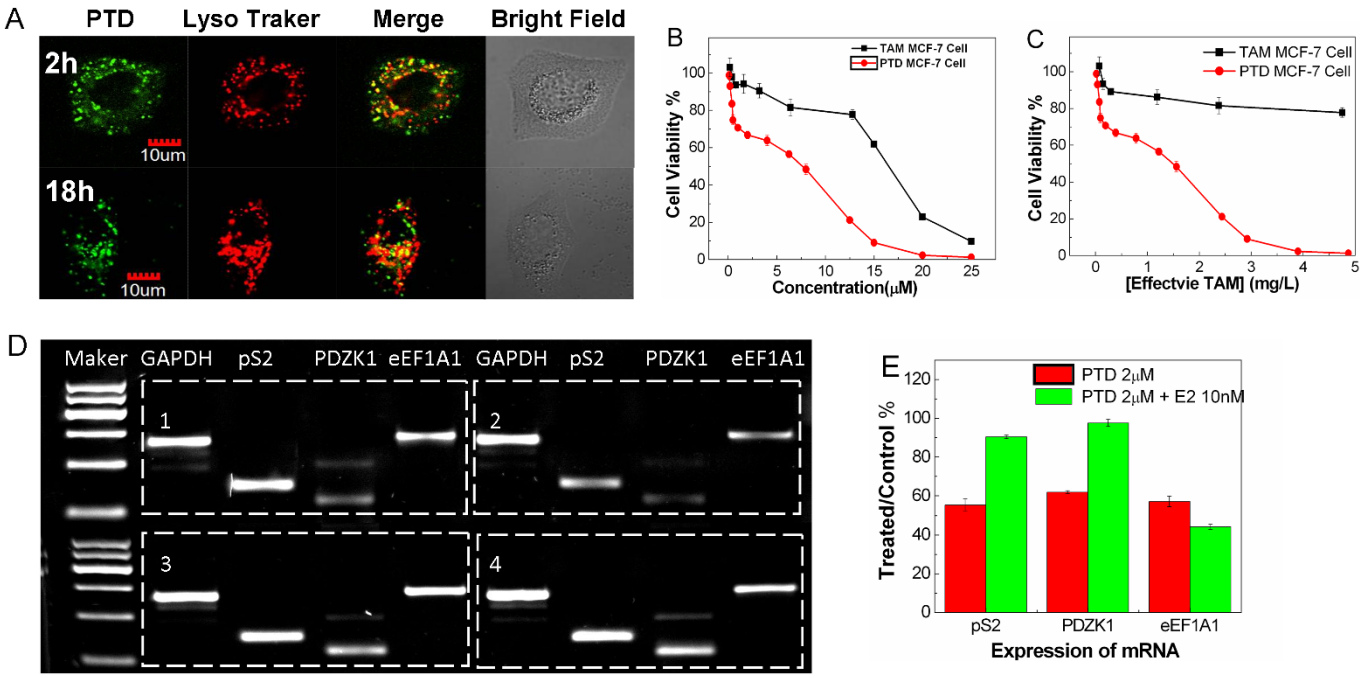

Figure 5 | (A) The cellular location of **PTD** at different incubation time: 2 h (upper) and 18 h (lower). The false color of **PTD** is green; the false color of Lyso Tracker DND 99 (lysosome stain) is red; their merge is yellow. (B, C) Dose-response curves for cell viability of MCF-7 Cells treated with tamoxifen or **PTD** as functions of **PTD** molar concentration (A) or mass concentration of effective **TAM** (B). (D) Reverse transcriptase-PCR analysis of mRNA. Images of DNA gel electrophoresis after reverse transcription-PCR reaction. After seeded for 12 h, MCF-7 cells are incubated under dark, group 1: without addition for 34 h; group 2: with **PTD** for 34 h; group 3: without addition for 24 h, and then with 10 nM 17-β-estrodiol for 10 h; group 4: with **PTD** for 24 h and then 10 nM 17-β-estrodiol added for 10 h. The housekeeping gene GAPDH is used as the internal reference. (E) Semi-quantitative analysis of mRNA expression. Red: group 1 as control and group 2 as treated; green: group 3 as control and group 4 as treated. Error bars correspond to standard deviations from three separate measurements.

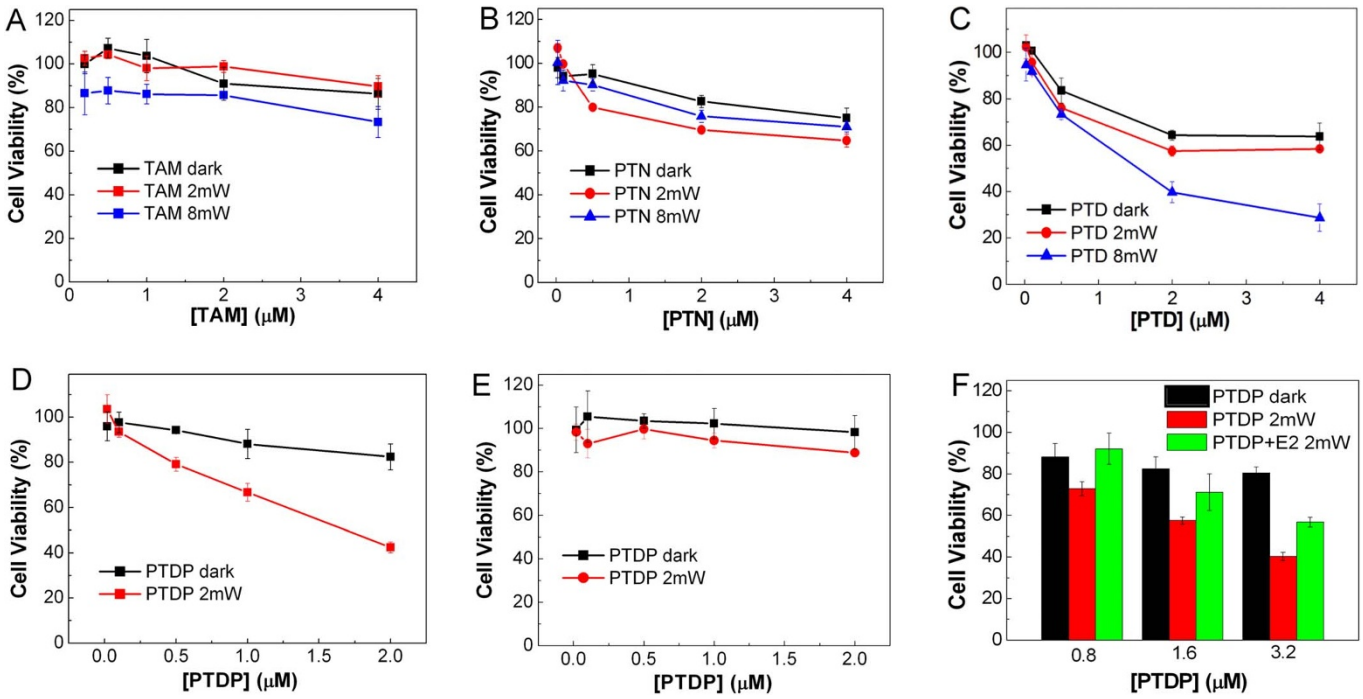

Figure 6 | **Dose-response curves for cell viability of MCF-7 cells treated with TAM (A), PTN (B) and PTD (C) by using a typical MTT assay under light irradiation or in the dark.** Dose-response curves for cell viability of MCF-7 cells (D) and MDA-MB-231 cells (E) treated with PTDP by using a typical MTT assay under light irradiation or in the dark. (F) Cell viability of MCF-7 cells treated with **PTDP** in the dark, under light irradiation or under light irradiation with 17-β-estrodiol added. The the 17-β-estrodiol with identical concentration to **PTDP** was added 2h before irradiation. Cells were irradiated with white light (400–800 nm). The concentrations of polymer are in RUs. Error bars correspond to standard deviations from three separate measurements.

Table 1 | Comparison of PTD and PTDP for inhibition activity to cell growth

		PTD (μM)			PTDP (μM)	
		1.0	2.0	4.0	1.0	2.0
Cell Viability (%)	dark	78	65	64	88	82
	2 mW	70	57	58	65	40
	8 mW	62	40	35	/	/

inhibition will contribute to the development of molecular targeted photodynamic therapy and new strategy of tumor treatment.

Methods

Materials and instruments. Tamoxifen was purchased from Beijing Zhongsheng Huateng technology (Beijing, China) and confirmed by ^{1}H NMR. 17-β-estrodiol was purchased from Aladdin. Other chemicals were purchased from Acros, Aldrich Chemical Company or Alfa-Aesar and used without purification. All organic solvents were purchased from Beijing Chemical Works and used as received. MCF-7 and MDA-MB-231 cell lines were obtained from cell culture center of Institute of Basic Medical Sciences, Chinese Academy of Medical Sciences (Beijing, China). Fetal bovine serum (FBS) was purchased from Sijiqing Biological Engineering Materials (Hangzhou, China). Dulbecco's modified Eagle medium (DMEM) and L-15 medium (Leibovitz) were purchased from HyClone/Thermofisher (Beijing, China). RNAprep pure Cell/Bacteria Kit and Quant Script RT Kit were purchased from Tiangen Biotech (Beijing, China). The absorbance for MTT analysis was recorded on a microplate reader (BIO-TEK Synergy HT, USA) at a wavelength of 570 nm. Water used in cell culture was purified by a Millipore filtration system. The^{1}H NMR and ^{13}C NMR spectra were recorded on a Bruker Avance 400 MHz spectrometer. Mass spectra were recorded on a Waters GCT spectrometer for high resolution mass spectra (HRMS), a SHIMADZU LCMS-2010 spectrometer for ESI. Elemental analyses were carried out with a Flash EA1112 instrument. UV-Vis absorption spectra were taken on a JASCO V-550 spectrophotometer. Fluorescence spectra were measured on a Hitachi F-4500 fluorometer equipped with a xenon lamp excitation source. The images of gel electrophoresis were taken by a Bio-Rad Molecular Imager ChemiDoc XRS system and quantitative analysis data were obtained using Quantity One software (Version 4.6.5). Confocal laser scanning microscopy (CLSM) characterization was conducted with a confocal laser scanning biological microscope (FV1000-IX81, Olympus, Japan). The white light source (400–800 nm) was provided by a metal halogen lamp (MVL-210, Mejiro Genossen, Japan). The intensity of the incident beam was determined by a radiometer (Photoelectric Instrument Factory (Beijing Normal University). The size of polymer systems was measured on a Nano ZS (ZEN3600) system.

Synthesis of 2-(thiophen-3-yl)ethyl 4-methylbenzenesulfonate (2). To dichloromethane (40 mL), 2-(thiophen-3-yl)ethanol (5.1 g, 40 mmol) and pyridine (4.0 g, 50 mmol) were added and the mixture was kept in 0°C. 4-methylbenzene-1-sulfonyl chloride (9.5 g, 50 mmol) in dichloromethane (20 mL) was then added slowly. The mixture was stirred for 24 h under room temperature. After that, the mixture was washed with excess HCl solution, and then dried over $MgSO_4$. The solvent was removed and the residue was purified by silica gel column chromatography using petroleum ether/ethyl acetate (10:1) as the eluent to afford a white solid (10.7 g, 95%). ^{1}H NMR (400 MHz, $CDCl_3$, δ): 7.74 (d, 2H), 7.32(d, 2H), 7.24(dd, 1H), 6.98 (d, 1H), 6.88 (d, 1H), 4.23 (t, 2H), 3.01 (t, 2H), 2.46 (s, 3H).

Synthesis of 3-(2-(2-(2-(2-(2-hydroxyethoxy)ethoxy)ethoxy)ethoxy)ethylthiophene (3). To a solution of sodium hydride (60% in oil dispersion, 3.0 g, 75 mmol) in anhydrous THF (60 ml) was added tetraethylene glycol (14.5 g, 75 mmol) drop by drop. After stirring at room temperature for 30 min, compound **2** (7.0 g, 25 mmol) in anhydrous THF was added to the mixture and allowed to react at 40°C for 12 h. The resulting mixture was quenched by distilled water and extracted with $CHCl_3$ three times. The combined organic layer was washed with water. Then the solvent was removed and the residue was purified by silica gel chromatography using petroleum ether/ dichloromethane/ethyl acetate/dimethoxyethylene (10:10:10:1) as the eluent to afford a colorless oil (1.5 g, 20%). ^{1}H NMR (400 MHz, $CDCl_3$, δ): 7.21 (dd, 1H), 7.00 (d, 1H), 6.95 (d, 1H), 3.56-3.72 (m, 18H), 2.90 (t, 2H). 13C NMR (100 MHz, $CDCl_3$, δ): 139.1, 128.4, 125.1, 121.1, 72.51, 71.40, 70.53, 70.48, 70.22, 70.14, 61.61, 30.52. HRMS (ESI) *m/z:* $[M+H]^+$ calcd. 305.1417; found 305.1411.

Synthesis of 14-(thiophen-3-yl)-3,6,9,12-tetraoxatetradecyl 4-methylbenzenesulfonate (4). To dichloromethane (30 mL), compounds **3** (2.0 g, 6.5 mmol) and pyridine (2.0 g, 26 mmol) were added and the mixture was kept in 0°C. 4-methylbenzene-1-sulfonyl chloride (2.5 g, 13 mmol) in dichloromethane (20 mL) was then added slowly. The mixture was stirred for 48 h under room temperature. After that, the mixture was washed with excess HCl solution, and then dried over Na_2SO_4. The solvent was removed and the residue was purified by silica gel column chromatography using petroleum ether/ethyl acetate/dimethoxyethylene (30:10:1) as the eluent to afford a colorless oil (2.4 g, 80%). ^{1}H NMR (400 MHz, $CDCl_3$, δ): 7.77 (d, 2H), 7.32 (d, 2H), 7.22 (dd, 1H), 7.01 (d, 1H), 6.96 (d, 1H), 4.14 (t, 2H), 3.56–3.72 (m, 16H), 2.89 (t, 2H), 2.42(s, 3H). ^{13}C NMR (100 MHz, $CDCl_3$, δ):144.9, 139.3, 133.1, 129.9, 128.6, 128.1, 125.3, 121.2, 71.58, 70.87, 70.71, 70.65, 70.34, 69.35, 68.79, 30.76, 21.77. ESI-MS *m/z*: $[M+Na]^+$ calcd. 481.1; found 481.2. $C_{21}H_{30}O_7S_2$: calcd. C 55.00, H 6.59; found C 54.84, H 6.58.

Synthesis of compound 5. To a solution of sodium hydride (60% in oil dispersion, 200 mg, 5 mmol) in anhydrous THF (30 mL) was added tetraethylene glycol (1.4 g, 7.5 mmol) drop by drop. After stirring at room temperature for 30 min, compound **4** (1.1 g, 2.5 mmol) in anhydrous THF was added to the mixture and allowed to react at 40°C for 12 h. The resulting mixture was quenched by distilled water and extracted with $CHCl_3$ three times. The combined organic layer was washed with water. Then the solvent was removed and the residue was purified by silica gel chromatography using petroleum ether/ethyl acetate/methanol/dimethoxyethylene (10:30:1:1) as the eluent to afford a colorless oil (600 mg, 50%). ^{1}H NMR (400 MHz, $CDCl_3$, δ): 7.24 (dd, 1H), 7.01 (d, 1H), 6.96 (d, 1H), 3.55–3.72 (m, 34H), 2.92 (t, 2H) 2.51 (br, 1H). ^{13}C NMR (100 MHz, $CDCl_3$, δ): 139.3, 128.6, 125.4, 121.2, 72.64, 71.60, 70.70, 70.46, 70.35, 69.59, 61.86, 30.76. HRMS (ESI) *m/z:* $[M+H]^+$ calcd. 481.2466; found 481.2462.

Synthesis of compound 6. To dichloromethane (8 mL), compounds **5** (500 mg, 1.0 mmol) and pyridine (420 mg, 5.2 mmol) were added and the mixture was kept in 0°C. 4-methylbenzene-1-sulfonyl chloride (570 mg, 3 mmol) in dichloromethane (2 mL) was then added slowly. The mixture was stirred for 48 h under room temperature. After that, the mixture was neutralized with HCl solution, and then dried over Na_2SO_4. The solvent was removed and the residue was purified by silica gel column chromatography using petroleum ether/ dichloromethane/ethyl acetate/ dimethoxyethylene (10:10:10:1) as the eluent to afford a colorless oil (630 mg 95%). ^{1}H NMR (400 MHz, $CDCl_3$, δ): 7.79 (d, 2H), 7.34 (d, 2H), 7.24 (dd, 1H), 7.03 (d, 1H), 6.98 (d, 1H), 4.16 (t, 2H), 3.55–3.72 (m, 32H), 2.93 (t, 2H), 2.45 (s, 3H). ^{13}C NMR (100 MHz, $CDCl_3$, δ): 144.9, 139.3, 133.1, 129.9, 128.6, 128.1, 125.3, 121.2, 71.58, 70.87, 70.69, 70.34, 69.36, 68.79, 30.76, 21.76. ESI-MS *m/z:* $[M+K]^+$ calcd. 673.2; found 673.3. $C_{29}H_{46}O_{11}S_2$: calcd. C 54.87, H 7.30; found C 54.68, H 7.26.

Synthesis of compound 7. To a solution of compound **6** (516 mg, 0.8 mmol) in anhydrous acetone (25 mL) was added $LiBr\cdot H_2O$ (1.6 g, 1.6 mmol) under nitrogen. The mixture was stirred and reflux at 75°C for 12 h. The mixture was concentrated under vacuum and residue was purified by silica gel column chromatography using petroleum ether/ dichloromethane/ethyl acetate/dimethoxyethylene (10:10:10:1) as the eluent to afford a colorless oil (200 mg, 40%). ^{1}H NMR (400 MHz, $CDCl_3$, δ): 7.24 (dd, 1H), 7.02 (d, 1H), 6.97 (d, 1H), 3.81 (t, 2H), 3.55–3.72 (m, 34H), 3.47 (t, 2H), 2.92 (t, 2H). ^{13}C NMR (100 MHz, $CDCl_3$, δ): 139.3, 128.5, 125.2, 121.1, 71.50, 71.25, 70.70, 70.63, 70.28, 30.70, 30.30. ESI-MS *m/z:* $[M+NH_4]^+$ calcd. 560.2; found 560.3.

Synthesis of compound 8. To a solution of compound **6** (530 mg, 0.8 mmol) in anhydrous acetone (40 mL) was added NaI (1.2 g, 8 mmol) under Nitrogen. The mixture was stirred and refluxed at 75°C for 12 h. The mixture was concentrated under vacuum. Water was added and the mixture was extracted with CH_2Cl_2. The combined organic layer was dried over Na_2SO_4. The solvent was removed and the residue was purified by silica gel column chromatography using petroleum ether/ dichloromethane/ethyl acetate/dimethoxyethylene (10:10:10:1) as the eluent to afford a colorless oil (420 mg, 85%). ^{1}H NMR (100 MHz, $CDCl_3$, δ): 7.24 (dd, 1H), 7.02 (d, 1H), 6.97 (d, 1H), 3.74 (t, 2H), 3.56–3.72 (m, 30H), 3.25 (t, 2H), 2.92 (t, 2H). ^{13}C NMR (400 MHz, $CDCl_3$, δ): 139.3, 128.6, 125.3, 121.3, 72.09, 71.60, 70.71, 70.35, 30.76. HRMS (ESI) m/z: $[M+H]^+$ calcd. 591.1483; found 591.1479.

Synthesis of polymer 9. A suspension of anhydrous $FeCl_3$ (100 mg, 0.6 mmol) in $CHCl_3$ (15 mL) was stirred for 30 min at room temperature under nitrogen. To this suspension was added a solution of monomer **3** (20 mg, 0.067 mmol) and monomer **8** (44 mg, 0.075 mmol) in $CHCl_3$ (10 mL), and the resulting solution was stirred for 2 days at room temperature. The solvent was removed gently and the residue was dissolved with methanol. The solution that phosphorus pentoxide directly dissolved in water was added. After stirring for a while, the supernatant was collected and the precipitate was washed repeatedly by methanol. The combined solution was dried and the residue was dissolved in DMSO/H_2O (1:10). Then the solution was dialyzed through a membrane with a molecular weight cutoff of 3500 for 3 days to yield a red sticky substance (25 mg, 39%). ^{1}H NMR (400 MHz, $CDCl_3$, δ): 6.8–7.2 (br), 3.75 (t), 3.4–3.74 (br), 3.25 (t), 3.10 (br), 2.80–3.00 (br).

Synthesis of PTN. To a solution of **PTI** (7 mg) in THF (1 mL), trimethylamine (1 mL, 33% in methanol, 4.2 mmol) was added. The resulted solution was stirred for 72 h at 60°C with trimethylamine extra added due to the not well-sealed system. The solution was removed under vacuum. The residue was dissolved in water and then dialyzed through a membrane with a molecular weight cutoff of 3500 for 3 days to yield a red sticky substance (7 mg, 94%). ^{1}H NMR (400 MHz, $CDCl_3$, δ): 6.8–7.2 (br), 4.4 (br), 3.93 (br), 3.88(br), 3.75 (m), 3.43–3.74 (br), 3.30 (s), 3.03–3.23 (br), 2.50–2.80 (br).

Synthesis of PTD. To a solution of **PTI** (15 mg) in methanol/$CHCl_3$ (1:1, 3 mL), tamoxifen (125 mg, 0.33 mmol) was added. The resulted solution was stirred for 48 h at 72°C with solvent extra added. The solution was removed under vacuum and the

residue was dissolved in little $CHCl_3$. The solution was precipitated into petroleum ether repeatedly to remove the unreacted tamoxifen and yield a red sticky substance (21 mg, 95%).^{1}H NMR (400 MHz, $CDCl_3$, δ): 7.31 (m, 2H), 7.10–7.25 (m, 9H), 6.79 (d, 2H), 6.54 (d, 2H), 4.31 (br, 2H), 3.9–4.2 (br, 6H), 3.50–3.85 (br, 40H), 3.42 (br, 6H), 2.80–3.20 (br, 3H), 2.43 (q, 2H), 0.90 (t, 3H).

Synthesis of PTDP. A suspension of anhydrous $FeCl_3$ (100 mg, 0.6 mmol) in $CHCl_3$ (10 mL) was stirred for 30 min at room temperature under nitrogen. To this suspension was added a solution of monomer **3** (8 mg, 0.03 mmol), monomer **7** (22 mg, 0.04 mmol) and monomer **10** (4 mg, 0.004 mmol) in $CHCl_3$ (10 mL), and the resulting solution was stirred for 2 days at room temperature. The solvent was removed gently and the residue was dissolved with methanol and $CHCl_3$. The solution that directly dissolves phosphorus pentoxide in water was added. After stirring for a while, the organic layer was collected and the precipitate was treated three times repeatedly. The combined solution was dried under vacuum and the residue was added to a solution (methanol:$CHCl_3$ = 1:1, 3 ml) of tamoxifen (500 mg, 1.3 mmol) and KI (45 mg, 0.3 mmol). The resulted solution was stirred for 48 h at 72°C with solvent extra added. The solution was removed under vacuum and the residue was dissolved in little $CHCl_3$. The solution was precipitated into petroleum ether repeatedly to remove the unreacted tamoxifen, then dissolved in water and dialyzed through a membrane with a molecular weight cutoff of 3500 for 3 days to yield a red sticky substance (18 mg, 36%). ^{1}H NMR (400 MHz, $CDCl_3$, δ): 8.83 (br, 8H), 8.13 (br, 8H), 7.52 (br, 6H), 7.10–7.40 (m, 162H), 6.78 (d, 26H), 6.54 (d, 26H), 4.31 (br, 28H), 3.9–4.2 (br, 80H), 3.20–3.85 (br, 700H), 2.80–3.20 (br, 52H), 2.70 (s, 9H), 2.44 (t, 26H), 1.70–2.10 (br, 8H), 0.90 (t, 39H), −2.76 (s, 2H).

Cell culture. MCF-7 cells were cultured in DMEM and MDA-MB-231 cells were cultured in L-15 medium, supplemented with 10% FBS at 37°C in a humidified atmosphere containing 5% CO_2.

In vitro imaging and localization. MCF-7 cells were seeded in 35 mm culture plates at a density of approximately 10% per plate for 24 h and then the culture medium 2 mL with 5 μM PTD replaced. After the cells were further culture for 1 h or 17 h, Lyso Traker DND 99 was added with a final concentration of 200 nM. After further culture for 1h, culture medium was discarded, the plate was washed once by PBS and fresh DMEM medium was added. Then the sample was characterized using CLSM. The wavelength of stimulating laser of PTD is 404 nm and that of Lyso Traker DND 99 is 559 nm. The false color of PTD is green and the false color of Lyso Traker DND 99 is red.

ROS measurements. The final concentration of DCFH was 40 μM. To 1.0 mL of the activated DCFH solution were added compounds. The fluorescence spectra were measured after the specimens were irradiated with white light (10 mW·cm^{-2}). Fluorescence spectra of DCF solution was recorded in 498–700 nm emission range with the excitation wavelength of 488 nm.

Reverse transcription PCR. MCF-7 cells in one group were treated with or without PTD for 34 h under dark. In another group, after cells were treated with or without PTD for 24 h, 17-β-estrodiol was added to the culture medium and the incubation was continued for 10 h. Total cellular RNA was extracted from cells with RNAprep pure Cell/Bacteria Kit and quantified by UV absorbance spectroscopy. The reverse transcription reaction was performed using the QuantScript RT Kit in a final volume of 20 μL containing 2 μg total RNA. After incubation at 37°C for 60 minutes, the reverse transcription was terminated. The 25 μL reaction mixture contained 2 μL cDNA as template. Primers used for GAPDH amplification were: (sense, 5′-ACAG-TCCATGCCATCACTGCC-3′; reverse, 5′-GCCTGCTTCACCACCTTCTTG-3′; 266 bp). Primers for pS2 amplification were: (sense, 5′-ATACCATCGACGTC-CCTCCA-3′; reverse, 5′-AAGCGTGTCTGAGGTGTCCG-3′; 147 bp). Primers used for PDZK1 amplification were: (sense, 5′-GAATCCAGAGCAGTGGGAAG-3′; reverse, 5′-AGGGTGTCAAGTGGATCAG-3′; 119 bp). Primers for eEF1A1 amplification were: (sense, 5′-TCGGGCAAGTCCACCACTAC-3′; reverse, 5′-GCACAGTCAGCCTGAGATGTC-3′; 284 bp). Amplification cycles were: 95°C for 4 min, the 30 cycles at 95°C for 30 s, 60°C for 30 s, 72°C for 30 s; followed by 72°C for 10 min. Amplification products with same volume were loaded on 3.5% agarose gel stained with Goldview DNA dye. Gels were run at 100 mA for 26 min and visualized in Bio-Rad Molecular Imager ChemiDoc XRS system. DNA bands were quantified by Quantity One software.

Cell growth inhibition assay. The stock solutions of tamoxifen, 17-β-estrodiol and 10 were prepared in ethanol. The final concentration of ethanol in the culture medium is below 0.1%, which hardly induce any cytotoxicity. All the polymers were directly dissolved in sterile water. In all the experiments, MCF-7 cells were seeded in 96-well U-bottom plates at a density of 7×10^3 cells/well while MDA-MB-231 cells at a density of 1.5×10^4 cells/well. After 12 h, cells were incubated with various concentrations of compounds in fresh medium. Followed by 48 h incubation, MTT (5 mg mL^{-1} in water, 10 μL/well) was added to the wells by incubation at 37°C for 4 h. The supernatant was removed and 100 μL DMSO per well was added to dissolve the produced formazan. After shaking the plates for 10 min, absorbance values of the wells were recorded with a microplate reader at 570 nm.

In the experiments of PDT, PDT treatment was performed 30 hours before MTT was added by using white light source at fluence rates of 2 mW·cm^{-2} or 8 mW·cm^{-2} for 30 min. In the experiments to test the reverse ability to PDT-induced growth inhibition, 17-β-estrodiol was added into the culture medium containing PTDP 2 hours before PDT treatment, with the concentration equal to PTDP. The control group was carried out with equal water added. All the data have been corrected with the data from zero poles.

1. Kyriakis, J. M. & Avruch, J. Mammalian mitogen-activated protein kinase signal transduction pathways activated by stress and inflammation. *Physiol. Rev.* **281**, 807–869 (2001).
2. Pawson, T. Protein modules and signaling networks. *Nature* **373**, 573–580 (1995).
3. Reya, T. & Clevers, H. Wnt signalling in stem cells and cancer. *Nature* **434**, 843–850 (2005).
4. Downward, J. Targeting ras signalling pathways in cancer therapy. *Nat. Rev. Cancer* **3**, 11–22 (2003).
5. Larsen, J. E., Cascone, T., Gerber, D. E., Heymach, J. V. & Minna, J. D. Targeted therapies for lung cancer clinical experience and novel agents. *Cancer J.* **17**, 512–527 (2011).
6. Hait, W. N. Targeted cancer therapeutics. *Cancer Res.* **69**, 1263–1267 (2009).
7. Moore, C. M., Pendse, D. & Emberton, M. Photodynamic therapy for prostate cancer-a review of current status and future promise. *Nat. Clin. Pract. Urol.* **6**, 18–30 (2009).
8. Bugaj, A. Targeted photodynamic therapy - a promising strategy of tumor treatment. *Photochem. Photobiol. Sci.* **10**, 1097–1109 (2011).
9. Tour, O., Meijer, R. M., Zacharias, D. A., Adams, S. R. & Tsien, R. Y. Genetically targeted chromophore-assisted light inactivation. *Nat. Biotechnol.* **21**, 1505–1508 (2003).
10. Service, R. F. Nanotechnology takes aim at cancer. *Science* **310**, 1132–1134 (2005).
11. Mitsunaga, M. *et al.* Cancer cell-selective in vivo near infrared photoimmunotherapy targeting specific membrane molecules. *Nat. Med.* **17**, 1685–U210 (2011).
12. Xing, C., Liu, L., Yang, Q., Wang, S. & Bazan, G. C. Design guidelines for conjugated polymers with light-activated anticancer activity. *Adv. Funct. Mater.* **21**, 4058–4067 (2011).
13. Lee, J., Udugamasooriya, D. G., Lim, H.-S. & Kodadek, T. Potent and selective photo-inactivation of proteins with peptoid-ruthenium conjugates. *Nat. Chem. Biol.* **6**, 258–260 (2010).
14. Rajfur, Z., Roy, P., Otey, C., Romer, L. & Jacobson, K. Dissecting the link between stress fibres and focal adhesions by CALI with EGFP fusion proteins. *Nat. Cell Biol.* **4**, 286–293 (2002).
15. Tanabe, T. *et al.* Multiphoton excitation-evoked chromophore-assisted laser inactivation using green fluorescent protein. *Nat. Methods* **2**, 503–505 (2005).
16. Marks, K. M., Braun, P. D. & Nolan, G. P. A general approach for chemical labeling and rapid, spatially controlled protein inactivation. *Proc. Natl. Acad. Sci. USA* **101**, 9982–9987 (2004).
17. Duan, X., Liu, L., Feng, X. & Wang, S. Assemblies of conjugated polyelectrolytes with proteins for controlled protein photoinactivation. *Adv. Mater.* **22**, 1602–1606 (2010).
18. Pecher, J. & Mecking, S. Nanoparticles of conjugated polymers. *Chem. Rev.* **110**, 6260–6279 (2010).
19. Chemburu, S. *et al.* Light-induced biocidal action of conjugated polyelectrolytes supported on colloids. *Langmuir* **24**, 11053–11062 (2008).
20. Corbitt, T. S. *et al.* Conjugated polyelectrolyte capsules: light-activated antimicrobial micro "roach motels". *ACS Appl. Mater. Interfaces* **1**, 48–52 (2009).
21. Ding, L. P. *et al.* Insight into the mechanism of antimicrobial conjugated polyelectrolytes: lipid headgroup charge and membrane fluidity effects. *Langmuir* **26**, 5544–5550 (2010).
22. Xing, C., Xu, Q., Tang, W., Liu, L. & Wang, S. Conjugated polymer/porphyrin complexes for efficient energy transfer and improving light-activated antibacterial activity. *J. Am. Chem. Soc.* **131**, 13117–13124 (2009).
23. Zhu, C. *et al.* Multifunctional cationic poly(p-phenylene vinylene) polyelectrolytes for selective recognition imaging and killing of bacteria over mammalian cells. *Adv. Mater.* **23**, 4805–4810 (2011).
24. Rickert, E. L. *et al.* Synthesis and characterization of fluorescent 4-hydroxytamoxifen conjugates with unique antiestrogenic properties. *Bioconjugate Chem.* **21**, 903–910 (2010).
25. MacGregor, J. I. & Jordan, V. C. Basic guide to the mechanisms of antiestrogen action. *Pharmacol. Rev.* **50**, 151–196 (1998).
26. Salami, S. & Karami-Tehrani, F. Biochemical studies of apoptosis induced by tamoxifen in estrogen receptor positive and negative breast cancer cell lines. *Clin. Biochem.* **36**, 247–253 (2003).
27. Rickert, E. L. *et al.* Synthesis and characterization of bioactive tamoxifen-conjugated polymers. *Biomacromolecules* **8**, 3608–3612 (2007).
28. Rivera-Guevara, C. *et al.* Genomic action of permanently charged tamoxifen derivatives via estrogen receptor-α. *Bioorg. Med. Chem.* **18**, 5593–5601 (2010).

Acknowledgments

The authors are grateful to the National Natural Science Foundation of China (Nos. 21033010, 21003140, 90913014, 21021091) and the Major Research Plan of China (Nos. 2012CB932600, 2011CB935800, 2011CB932302).

Author contributions

B. W. designed experiments, conducted experiments and data analysis, and wrote the paper; H. Y. conducted experiments and data analysis; C. Z., Q. Y., L. L. and F. L. conducted data analysis; S.W. designed experiments, performed data analysis and wrote the paper.

Additional information

Competing financial interests: The authors declare no competing financial interests.

How to cite this article: Wang, B. *et al.* Polymer-drug conjugates for intracellar molecule-targeted photoinduced inactivation of protein and growth inhibition of cancer cells. *Sci. Rep.* **2**, 766; DOI:10.1038/srep00766 (2012).